J Solid State Electrochem (2006) 10: 104–109
DOI 10.1007/s10008-005-0675-5

ORIGINAL PAPER

A. Vadivel Murugan · B. B. Kale · Lalita B. Kunde
Aarti V. Kulkarni

Comparison of different soft chemical routes synthesis of nanocrystalline $LiMn_2O_4$ and their influence on its physicochemical properties

Received: 5 November 2004 / Revised: 24 February 2005 / Accepted: 9 March 2005 / Published online: 12 May 2005

Abstract A comparative study of nanocrystalline spinel $LiMn_2O_4$ powders prepared by two different soft chemical routes such as solution and sol-gel methods using lithium and manganese acetates are the precursors under different calcination temperatures. The dependence of the physicochemical properties of the spinel $LiMn_2O_4$ powder has been extensively investigated by using thermal analysis (TGA/DTA), FTIR, X-ray diffraction studies, SEM, specific surface area (BET) and electrical conductivity measurements. The results show that pure $LiMn_2O_4$ can be prepared from acetate precursors as starting materials at a low temperature of 600°C from solution route and 500°C from sol-gel method. The charge-discharge characteristics and the cycling behavior of Li/1M $LiBF_4$-EC/DEC electrolyte / $LiMn_2O_4$cells revealed that $LiMn_2O_4$ calcined at higher temperatures showed a high initial capacity, while the $LiMn_2O_4$calcined at lower temperatures exhibited a good cycling behavior.

Keywords Spinel $LiMn_2O_4$ · Sol-gel · Solution · Cathode materials · Lithium batteries

Introduction

At present, lithium manganese oxide-based materials are among the most extensively studied promising cathode materials in lithium rechargeable batteries for portable electronic devices [1, 2]. The main advantages of choosing this cathode material for lithium batteries are abundance of manganese, cost-effective and eco-friendly characteristics [3]. At room temperature, $LiMn_2O_4$ shows a cubic spinel-type structure, *Fd3m* space group. The structure can be described as ideally consisting of a cubic close-packed arrangement of oxygen ions at 32e sites, the Li^+ ions occupy the tetrahedral 8a sites and the Mn^{3+} and Mn^{4+} ions octahedral 16d sites. In the cubic phase, lithium extraction/insertion from into the tetrahedral 8a sites occurs at 4V, it is associated with the $Mn^{3+} \leftrightarrow Mn^{4+}$ oxidation and reduction process [4–7]. Conventionally, lithium manganese oxide powders are synthesized by a solid-state reaction of lithium and manganese salts [8, 9] have several disadvantages such as inhomogeneity, irregular morphology, larger particle size, poor control of stoichiometry and longer period of calcinations followed by grinding; hence, other techniques are employed. Recently, various wet chemical methods have been reported with several advantages such as good homogeneity, low calcination temperatures with uniform sub-micron size particles, which is an important factor in achieving high battery performance. [10–12]. Indeed, the novel preparation techniques have expanded in such a way that several recent reports focused only on specific soft chemical routes, particularly on the possibility of enhancing the electrochemical properties of rechargeable lithium batteries. In this present communication, comparative studies of lithium manganese oxide, spinel powders have been synthesized by both the solution route as well as the sol-gel method. The effect of different calcination temperatures on the physicochemical properties and electrochemical behavior of $LiMn_2O_4$has been investigated. We observed that the phase pure $LiMn_2O_4$ formed at low temperature at 300°C when prepared by sol-gel method as compared to solution route synthesis at 600°C, and also with different morphological structure by which $LiMn_2O_4$has been prepared from different soft chemistry routes. The high initial capacity and good cycling behavior of the $LiMn_2O_4$ powder were closely related to the higher crystallinity and retention of the spinel structure.

A. Vadivel Murugan (✉) · B. B. Kale · L. B. Kunde
A. V. Kulkarni
Centre for Materials for Electronics Technology (C-MET),
Department of Information Technology, Government of India,
Panchawati, Off-Pashan Road, Pune, 411008, India
E-mail: avm@cmetindia.org
Tel.: +91-020-25898390
Fax: +91-020-25898180

Experimental

A stoichiometric amount of Lithium Acetate (99.5%,Aldrich) and Manganous Acetate (99%, Aldrich) salts with the cationic ratio of Li:Mn i.e. 1:2 was dissolved in methanol and mixed well with a small amount of citric acid as a chelating agent. After stirring continuously for 1 h, the solution was evaporated at 60°C in a water bath to form a transparent sol and subsequently the sol became an homogeneous transparent pink gel after 12 h. It is believed that the carboxylic acid group in the citric acid forms a chemical bonding with metal ions so that they become an extremely viscous gel [13–15]. The gel obtained was dried at 300°C for 10 h in air to eliminate organic contents. The powders were slightly ground and calcined to 300–600°C for 10 h in air to obtain phase-pure nanocrystalline $LiMn_2O_4$. In the solution route, acetate precursors of lithium and manganese were dissolved in water. After stirring continuously for 1 h, the homogeneous solution obtained was evaporated at 80°C. The as-synthesized metal acetate powders were calcined to 300–600°C for 10 h in air to obtain phase-pure crystalline $LiMn_2O_4$ powder. Thermal decomposition behavior of the gel precursor was examined by means of the Thermogravimetric Analyzer (Shimadzu TGA-50) and powder X-Ray diffraction (Bruker AXS D 5005) using Cu-Kα radiation to identify the crystalline phase of the materials calcined at various temperatures. Electron micrograph (SEM) images were taken on a Philips XL-30 equipment after mounting samples on Al stubs with gold coatings. The specific surface area of the material was measured by the BET method with nitrogen adsorption. Electronic conductivity measurements were made on compaction of powder in pellet form by using four-point probe conductivity method. The electrochemical properties of $LiMn_2O_4$ powder were determined in three-electrode electrochemical cell. The reference and counter electrodes were constructed from the Lithium foil (Aldrich 99.9%).The electrolyte used was a mixture of diethyl carbonate and ethylene carbonate containing 1 M $LiBF_4$. The cathode was a mixture of 80 wt% active material, 15 wt% of carbon black and 5 wt% of teflon binder. Thereafter, the cells were assembled in an argon-filled dry box, the charge–discharge cycling was galvanostatically performed at a current density of 1 mA/cm^2 (at the rate of 0.5 C), with cut-off voltage of 3.6 to 4.3 V (Vs Li/Li$^+$). Electronic conductivity measurements were made on compactions of powder in pellet form by using a four-probe conductivity method.

Result and discussion

The TGA/DTA plot of metal acetate powders and gel precursor that were obtained from both solution route and sol–gel methods are shown in Fig. 1 a, b respectively, which indicates the formation of $LiMn_2O_4$, which occurs at 310°C, for acetate precursor. The formation of $LiMn_2O_4$ is accompanied by the highly exothermic decomposition of organic groups in the presence of acetate precursors in the case of sol-gel powder. Figure 2a, b shows X-ray diffraction pattern for the solution and sol-gel derived materials, respectively, calcinated at various temperatures for 10 h in air. For the solution-derived material calcinated at 300°C, the crystallinity of $LiMn_2O_4$ spinel phase was not clear but the peaks of impurities such as Li_2CO_3, MnO_2, Mn_2O_3 and acetate were observed. Significantly, the same impurity peaks were not observed in the case of sol-gel derived materials calcinated at 300°C, which are often found in other low-temperature techniques. There may be co-ordination of acetates with metals in the gel network in methanol, which after oxidation gives respective carboneous gases. These XRD analysis showed a single phase of spinel-$LiMn_2O_4$ exhibiting the *Fd3m* space group with the lattice parameters a = 8.194 Å for 300°C, 8.201 Å for 500°C and 8.234 Å for 600°C respectively. The expansion of lattice parameter with increasing the annealing temperature may be attributed to the dilatational strains [16] resulting from the existence of Li vacancies, since the lattice parameters increase slightly with increasing the annealing temperature and time, which could be connected with Li evaporation

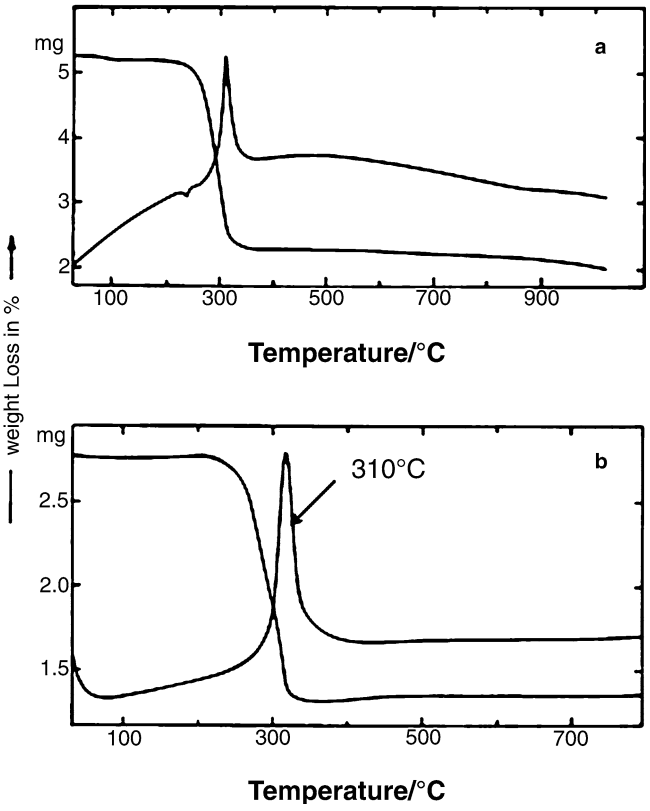

Fig. 1 TGA/DTA plot of **a** solution route and **b** sol-gel derived acetate precursors of nanocrystalline $LiMn_2O_4$ at the heating rate of 10°C/min

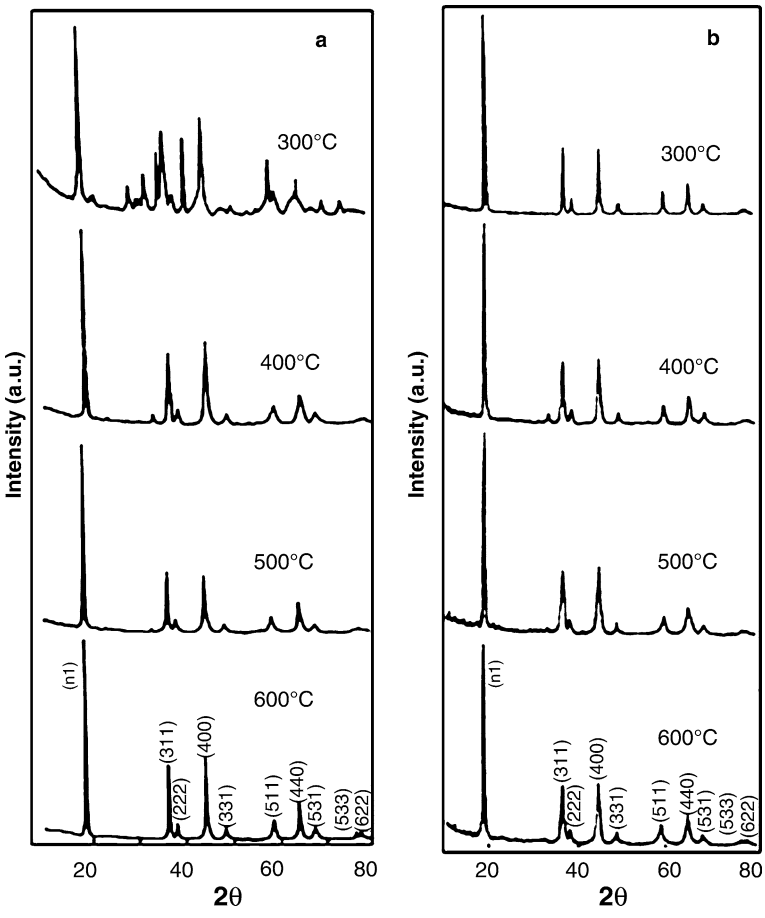

Fig. 2 XRD patterns of nanocrystalline $LiMn_2O_4$ precursors obtained from **a** solution route and **b** sol-gel method calcinated at different temperatures

[17]. It is very interesting to note that the (220) diffraction line that originated only from the tetrahedral Li-ion site in the spinel structure, is not observed in our materials. This means that manganese ions are not displaced into tetrahedral sites and only Li-ions with very small scattering factor, occupy the sites [10]. On the other hand, the sharper the intensities of diffraction peaks, the better the crystallinity of the $LiMn_2O_4$ spinel phase was from both the solution route and sol-gel method at higher calcination temperatures from 400°C to 600°C. In particular, the (533) and (622) reflections were diffused with increasing the annealing temperature. The precursors were transformed into phase pure $LiMn_2O_4$ crystalline spinel powders without any development of minor phase during calcinations at different temperatures. These results strongly suggest that these synthetic methods such as solution and sol-gel routes are much superior to the solid state reaction, since phase-pure $LiMn_2O_4$ spinel powders are prepared at much lower calcination temperatures in a shorter calcination time. The average grain size of the materials was calculated from the Scherer formula by full width at the half maximum (FWHM) at the (400) peak at 2θ 44°. Significantly, linear crystallite growth was observed with increasing calcinations temperature from 300°C to 600°C. In addition, the FTIR spectra of lithium manganese acetate precursors derived from both the solution route and the sol-gel method that are heated at different temperatures from 300°C to 600°C are illustrated in (Fig. 3 a, b) respectively. With increasing the calcinations temperature from 300°C to 600°C, the carboxylic (acetate) υ CO peaks at 1,330–1,670 cm^{-1} disappears and the characteristic peaks of $LiMn_2O_4$ gradually develop and peaks at 517 and 616 cm^{-1}, which are consistent with XRD result. Figure 4 a, b shows SEM micrographs of $LiMn_2O_4$ powders were prepared from both solution and sol-gel routes which were calcined at 600°C. It is interesting to observe the different morphologies of spherical $LiMn_2O_4$ from solution route and agglomerated rod like $LiMn_2O_4$ from sol-gel route. When the solution and sol-gel $LiMn_2O_4$precursors were calcined at 600°C, it was observed that the average particle size of the solution route powders increases upto 250 nm whereas in sol-gel, the particle size increases up to 119 nm with a narrow particle size distribution. Obviously, there is a decrease in particle size and change in morphology of $LiMn_2O_4$ prepared from sol-gel route as compared to solution route, which is also in good agreement with XRD. Figure 5 shows the comparative study of surface area (BET) dependence on the calcination temperature of lithium manganese acetate precursors derived from both solution route and sol-gel method. The specific surface area of the $LiMn_2O_4$ powders decreases linearly with increasing the

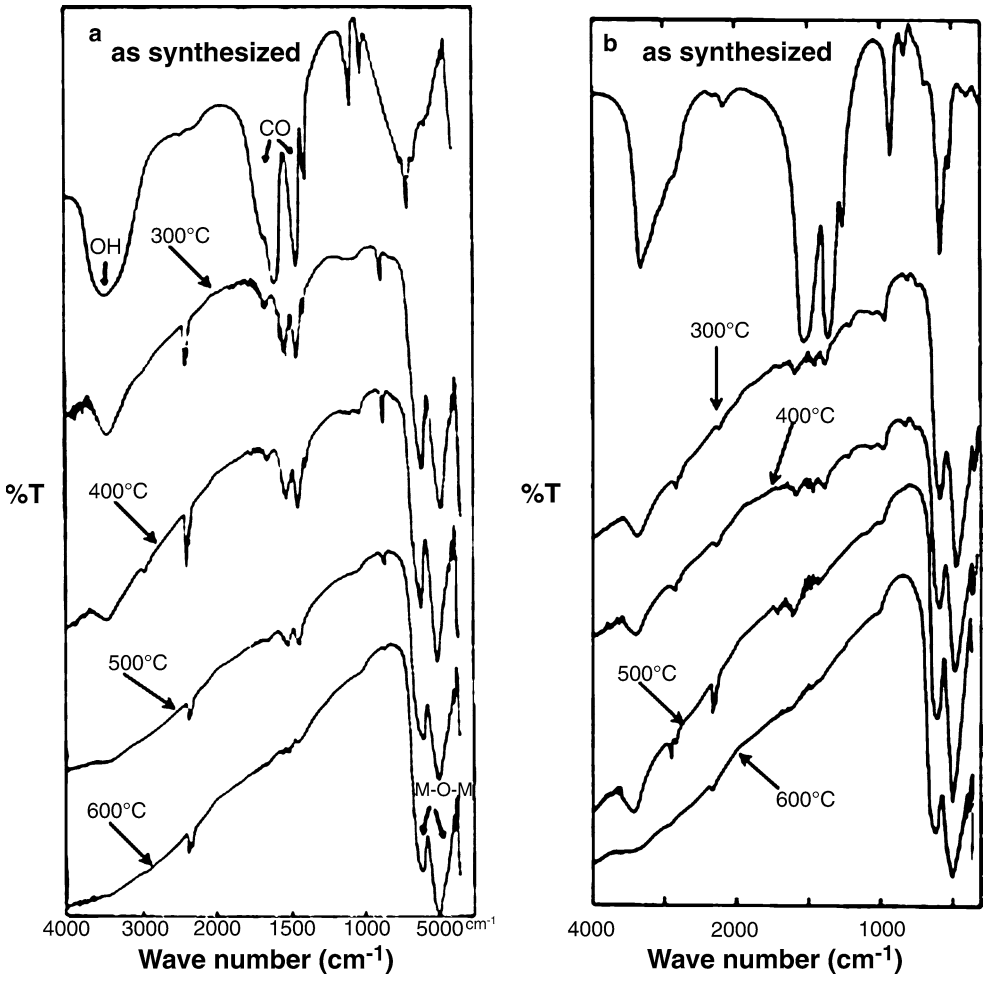

Fig. 3 FTIR spectra of nanocrystalline $LiMn_2O_4$ as synthesized precursors obtained from **a** solution route and **b** sol-gel method calcinated at different temperatures

calcinations temperature. This is mainly due to the growth of $LiMn_2O_4$ crystallite as observed in the dependence of crystallite size with the temperature. This is ascribed to the fact that the materials derived from the gel precursor consists of small-size particles since they are of atomic scale, and are homogeneously mixed with each other.

Four-probe electronic conductivity of $LiMn_2O_4$prepared from solution and sol-gel methods that have been studied in the temperature range of 300 K–573 K in air shows a linear increase in conductivity indicative of thermally activated electron transport behavior as shown in Fig. 6. Similar behavior has been observed of $LiMn_2O_4$ prepared by solid–solid state method reported recently [24]. The room temperature conductivity for $LiMn_2O_4$ had values typically in the range of 2.8×10^{-7} Scm^{-1}, whereas, the value obtained was 1.5×10^{-5} Scm^{-1} at 573 K. The electron transport behaviors slightly varied where $LiMn_2O_4$ was derived from these different methods as shown in Fig. 6. In addition, recent reports on thermoelectric measurements showed that $LiMn_2O_4$ is an n-type semiconductor [24] in which the electronic conductivity is due to electron hopping from the Mn^{3+} to the Mn^{4+} ions [18–24]. $LiMn_2O_4$undergoes a reversible cubic (*Fd3m*) ↔ orthorhombic (*Fddd*) phase transformation at temperatures close to room temperature. The phase transition is accompanied by a change in the electronic conductivity, which is lower for the low-temperature orthorhombic phase [20, 24]. Figure 7shows the voltage *vs* discharge capacity of the Li/1M $LiBF_4$-EC/DEC electrolyte/ $LiMn_2O_4$ cells with the cycle number (Fig. 8) at a constant charge discharge current density of 1 mA /cm^2 for $LiMn_2O_4$ powders prepared from both solution route and sol-gel method calcined at 300°C and 600°C. $LiMn_2O_4$ powders prepared from both solution and sol-gel method calcined at 300°C showed initial discharge capacity 87 and 95 $mAhg^{-1}$ respectively, whereas $LiMn_2O_4$ powders calcined at 600°C showed initial discharge capacity of 120 $mAhg^{-1}$, which is same for both routes. The capacity slowly decreases (Fig. 8) with respect to cycle number and remains at 82 and 93 $mAhg^{-1}$ at the 50th cycle for the $LiMn_2O_4$ powder calcined at 300°C obtained from both solution route and sol–gel method, respectively. Whereas in the case of $LiMn_2O_4$ powder obtained from solution route and sol-gel method calcined at 600°C showed the capacity to be 112 $mAhg^{-1}$. It is inferred from the above results that $LiMn_2O_4$ powder calcined at lower temperature have lower initial

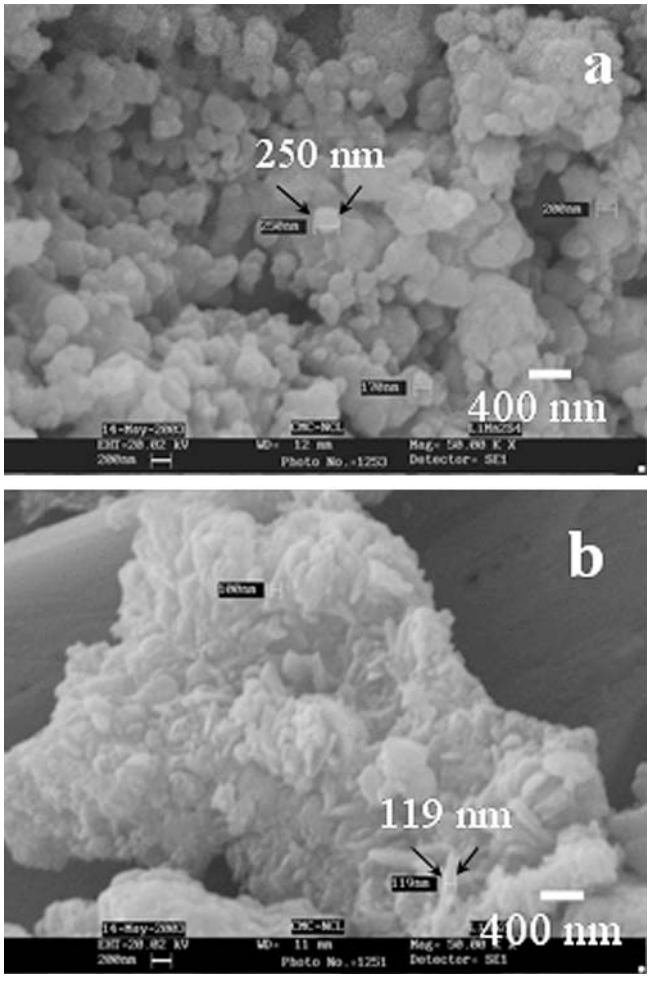

Fig. 4 SEM micrographs of Nanocrystalline $LiMn_2O_4$ prepared form **a** solution route **b** sol-gel method calcinated at 600°C for 10 h

capacity (95 $mAhg^{-1}$) and that when the same is calcined at higher temperatures they have higher crystallinity and thus higher initial capacity (120 $mAhg^{-1}$).

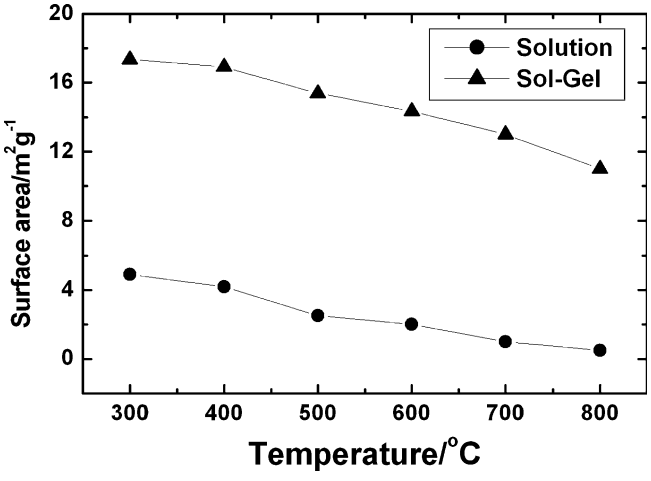

Fig. 5 Plot of surface area (BET) of the nanocrystalline lithium manganese oxide obtained from both solution route and sol-gel method at different calcination temperatures

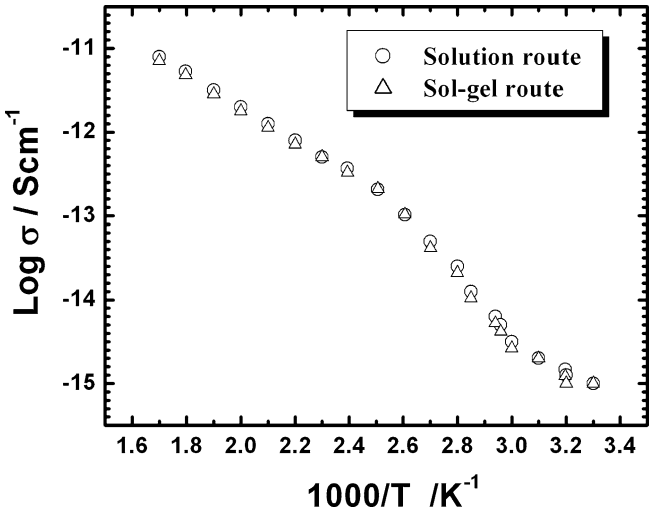

Fig. 6 Plot of conductivity (log σ) with reciprocal of temperature (1,000/T) of electron transport behavior of $LiMn_2O_4$ prepared form sol-gel and solution routes

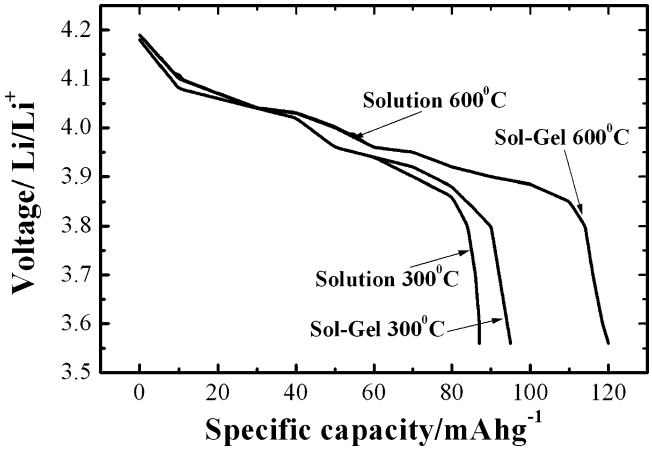

Fig. 7 First discharge curves for the Li/1M $LiBF_4$-EC/DEC electrolyte/$LiMn_2O_4$ cells using nanocrystalline $LiMn_2O_4$ powders obtained from solution route and sol–gel method calcinated at 300°C and 600°C. Cycling was carried out galvanostatically at constant charge–discharge current density of 1 mA/cm^2 between 3.6 V–4.3 V

The capacity fading observed after the 50th cycle, it may be due to Jahn-Teller distortion, which has been recently reported by Z.Jiang et al. [25].

Conclusion

The spinel $LiMn_2O_4$ powders with submicron narrow particle size distribution and excellent phase-pure particles were synthesized at 300 – 600°C for 10 hr in air by both solution route and sol–gel method using a non-aqueous solution of metal acetate containing citric acid as a chelating agent. We also observed that the phase-pure $LiMn_2O_4$ formed at low temperature at 300°C when prepared by sol-gel method as compared to the

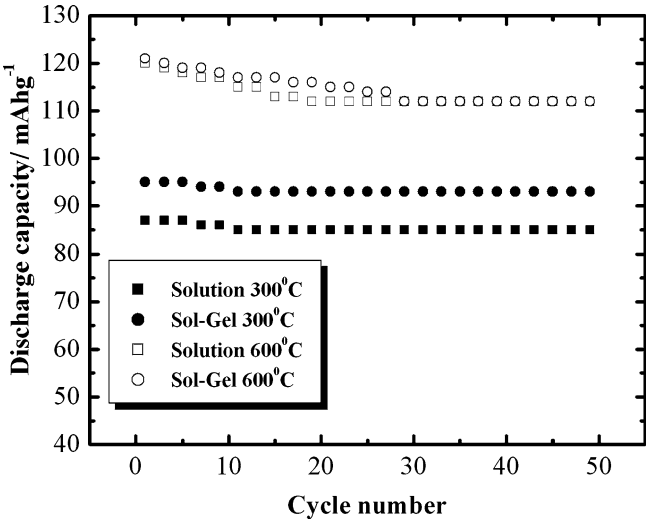

Fig. 8 Variation of specific discharge capacity with number of cycles for the Li/1M $LiBF_4$-EC/DEC electrolyte/$LiMn_2O_4$ cells using nanocrystalline $LiMn_2O_4$ powders obtained from both solution route and sol-gel method calcinated at 300°C and 600°C. Cycling was carried out galvanostatically at constant charge-discharge current density of 1 mA/cm^2 between 3.6 V and 4.3 V

solution route synthesis at 600°C and also with different morphological structure by which $LiMn_2O_4$ has been prepared from different soft chemistry routes. The crystallinity of $LiMn_2O_4$ powders increased with increase in calcination temperatures. The surface area decreased with increase in the temperature. The $LiMn_2O_4$powder with higher homogeneity in Li/1M $LiBF_4$-EC/DEC electrolyte/$LiMn_2O_4$cells had shown good discharge capacity and excellent cyclability. The high initial capacity and good cycling behavior of the $LiMn_2O_4$ powder were closely related to the higher crystallinity and retention of the spinel structure.

Acknowledgements Authors gratefully acknowledge Ministry of non-conventional energy sources (MNES), Goverment of India, New Delhi provided by the financial support [MNES (6/4/8/99-NT)] and would also like to thank Dr. B.K.Das, Executive Director, Dr. K. Vijayamohanan, Scientist, Physical and Materials Chemistry Division, NCL, Mr. S.K.Apte for FTIR analysis, Mr. R. Marimuthu for Thermogravimetric analysis from C-MET, Dr. Sainkar, NCL for SEM analysis.

References

1. Sun YK (1997) Solid State Ionics 100:115
2. Magahed S, Scrosati B (1994) J Power Sources 51:79
3. Yamada A, Miura K, Hinokuma K, Tanaka M (1995) J Electrochem Soc 142:2149
4. Guohua L, Ikuta H, Uchida T, Wakihara M (1996) J Electrochem Soc 143:178
5. Pistoia G, Antonini A, Rosati R, Bellitto C, Ingo GM (1997) Chem Mater 9:1443
6. Arora P, Popov BN, White RE (1998) J Electrochem Soc 145:807
7. Strowbel P, Ibarra Palos A, Anne M, Le Cras F (2000) J Mater Chem 10:429
8. Thackeray MM, Bruce PG, Goodenough JB (1984) Mater Res Bull 19:179
9. Nagaura T, Yokokawa M, Hasimoto T (1989) US Patent 4:828
10. Kushida K, Kuriyama K (2000) Appl Phys Lett 76:2238
11. Kang S-Ho, Goodenough JB, Rabenberg LK (2001) Chem Mater 13:1758
12. Choi S, Manthiram A (2000) J Electrochem Soc 147:1623
13. Baythoun MSG, Sale FR (1982) J Mater Sci 17:2757
14. Lessing PA (1989) Ceram Bull 68:1002
15. Liu W, Farrington GC, Chaput F, Dunn B (1996) J Electrochem Soc 143:879
16. Pankove JL (1975) Optical processes in semiconductors. Dover, New York
17. Pistoia G, Wang G (1993) Solid State Ionics 66:135
18. Goodenough JB, Manthiram A, Wnetrzewski P (1993) J Power Sources 43:269
19. Shimakawa Y, Numata T, Tabuchi J (1997) J Solid State Chem 131:138
20. Molenda J, Kucza W (1999) Solid State Ionics 117:41
21. Rousse G, Masquelier C, Rodriguez-Carvajal J, Hervieu M (1999) Electrochem Solid-State Lett 2:6
22. Rousse G, Masquelier C, Rodriguez-Carvajal J, Elkaim E, Lauriat JP, Martinez JL (1999) Chem Mater 11:3629
23. Massarotti V, Capsoni D, Bini M, Azzoni CB, Paleari A (1997) J Solid State Chem 128:80
24. Mandal S, Rojas RM, Amarilla JM, Calle P, Kosova NV, Anufrienko VF, Rojo JM (2002) Chem Mater 14:1598
25. Jiang Z, Abraham KM (1996) J Electrochem Soc 143:1591